

SERICITE AND INTERSTRATIFIED SERICITE-MONTMORILLONITE ASSOCIATED WITH KUROKO DEPOSITS IN THE HOKUROKU DISTRICT, JAPAN

SHOJI HIGASHI

Department of Geology, Kochi University, Kochi, Japan

(Received January 30, 1974)

ABSTRACT

Six specimens of sericite minerals collected from wall-rock alteration zones of the Kuroko deposits of the Hanaoka, Kosaka and Shakanai mines, Akita Prefecture, have been examined by x-ray, chemical, infrared absorption and differential thermal analyses. The results reveal that one specimen is sericite, and the other five are interstratified minerals of sericite and montmorillonite with 5 to 40 percent montmorillonite layers. Polytypes identified in the specimens are $2M_1$, 1M and 1Md.

Chemically the specimens are characterized by high aluminium and low magnesium and iron contents, and have a dioctahedral structure. The slight differences in octahedral composition due to substitution of aluminium by magnesium and iron can be correlated with their polytypes: the $2M_1$ type has a composition close to that of muscovite, but the 1M type is phengitic. The $d(060)$ spacings and the vibration frequencies of the IR bands at about 530 cm^{-1} also indicate these chemical variations. The differences in appearance of the endothermic peaks between 500° and 700°C of the DTA curves seem to be related to the octahedral composition.

INTRODUCTION

It is well known that the Kuroko deposits are accompanied by remarkable clayey alteration of wall rocks, and many kinds of clay minerals have been reported. However, mineralogical descriptions of sericite minerals which are the most prominent constituents of the alteration zone are rather few.

Recently, Shimoda (1970) found a dioctahedral mica with $2M_2$ structure from the Shakanai mine, and mineralogical studies were made on some sericite minerals (Shimoda, 1972; Shimoda and Nishiyama, 1973).

Shirozu and Higashi (1972) examined x-ray properties of sericite minerals which are distributed abundantly in and around the Kuroko deposits in the Hokuroku district, Akita Prefecture, and demonstrated that they comprise interstratified minerals of sericite and montmorillonite with various proportions of the component layers as well as pure sericite. This paper describes mineralogical properties of some of these sericite minerals.

MODES OF OCCURRENCE AND SPECIMENS

The present specimens were collected from the Hanaoka mine (Matsumine deposit), the Kosaka mine (Uwamuki deposit) and the Shakanai mine (No. 1 deposit) of Akita Prefecture. These deposits are typical Kuroko deposits consisting of three kinds of ores, namely, black ore (sphalerite-galena ore), yellow ore (pyrite-chalcopyrite ore) and silicified ore (quartz-pyrite ore). The wall rocks of the deposits are rhyolite, tuff, tuff breccia and mudstone, and they are intensely argillized, producing a large number of clay minerals (Shirozu and others, 1972). Sericite minerals are the most predominant constituent of the alteration products. Localities and modes of occurrence of six specimens examined are listed in Table 1.

TABLE 1. Localities and modes of occurrence of six specimens

Specimen	Locality	Description
M260-111	Matsumine deposit, 260m level.	White clay vein in silicified white rhyolite. Associated with euhedral pyrite and quartz.
Sh102	Shakanai mine, No. 1 deposit.	Hanging-wall white clay above a black ore body. Associated with barite.
K328-03	Uwamuki deposit, 30m level.	White clay matrix in the disseminated black ore (sphalerite and galena).
K329-12	Uwamuki deposit, 30m level.	Hanging-wall gray clay above a black ore body. Associated with fine-grained pyrite.
M180-29	Matsumine deposit, 180m level.	Hanging-wall white clay above a yellow ore body.
M165-10	Matsumine deposit, 165m level.	Hanging-wall pale gray clay above a black ore body.

These materials are fine-grained, and white or grayish clay with a weak silky luster. After ultrasonic dispersion, size fractionation at 2 microns was accomplished by a normal sedimentation method. The clay fraction thus obtained was free from impurities, and used for all the analyses.

X-RAY ANALYSIS

X-ray diffraction data were obtained with a Toshiba Model ADG-102 diffractometer, using $\text{CuK}\alpha$ radiation. Oriented aggregate prepared on slide glass was analysed in an air-dried state and after being subjected to glycerol solvation for 12 hours to examine the extent of intermixing of the expandable layer.

The proportions of the expandable layer were determined by examining the changes of line profile and the peak migrations after glycerol solvation and by referring to the curves of MacEwan and others (1961). The obtain-

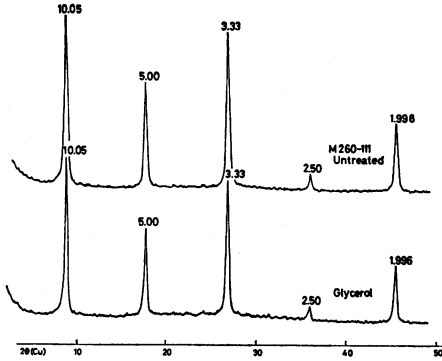


FIG. 1. X-ray diffraction patterns of specimen M260-111 (oriented aggregate).

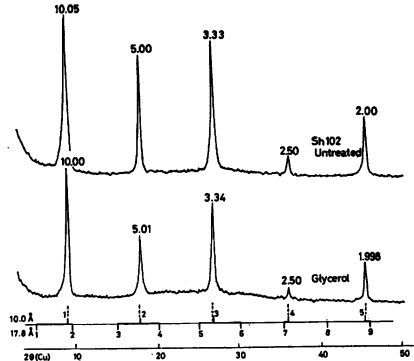


FIG. 2. X-ray diffraction patterns of specimen Sh 102 (oriented aggregate).

ed values are considered to be relative rather than absolute. X-ray pattern traces for the six specimens are given in Figs. 1 to 6.

The x-ray diffraction patterns of specimen M260-111 (Fig. 1) indicate that the specimen is exceptionally pure mica and contains no expandable layer. The basal reflections are symmetrical in profile and their spacings make an integral series of 10 Å. Specimen Sh102 also has sharp basal reflections in the air-dried state, but the glycerol treatment affects subtly the relative intensities of these reflections, particularly of the 002 reflection (Fig. 2). This change may be attributed to the existence of a small amount (about 5 percent) of an expandable layer. The asymmetrical and broad basal reflections in the air-dried state of specimen K328-03 together with their changes after glycerol solvation indicate that in a larger amount, presumably 5-10 percent, the expandable layer is intermixed in this specimen (Fig. 3).

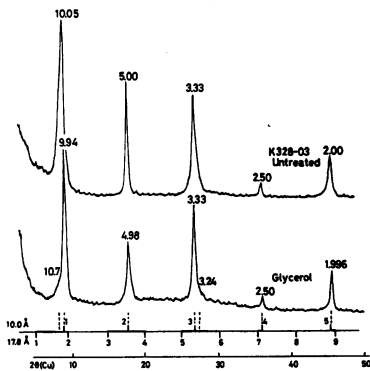


FIG. 3. X-ray diffraction patterns of specimen K328-03 (oriented aggregate).

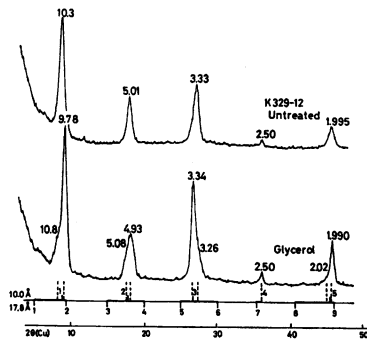


FIG. 4. X-ray diffraction patterns of specimen K329-12 (oriented aggregate).

The 001 spacings of specimens K329-12 and M180-29 are larger than 10 Å of pure mica phase, and the spacings of the higher order basal reflections do not form an integral series. By the glycerol treatment, these reflections split into two peaks, or shoulders appeared (Figs. 4 and 5). As indicated by the horizontal lines for visual inspection (Weaver, 1956), these changes can be interpreted as results of random interstratifications of two components, mica (10 Å) and expanded montmorillonite (17.8 Å). By averaging the proportions obtained from the spacings of the (001)₁₅/(001)₁₀ for the untreated samples and those of the (001)₁₀/(002)_{17.8}, (002)₁₀/(004)_{17.8} and (003)₁₀/(005)_{17.8} after glycerol solvation, 15 and 25 percent of layers are estimated to be montmorillonite layers in specimens K329-12 and M180-29, respectively.

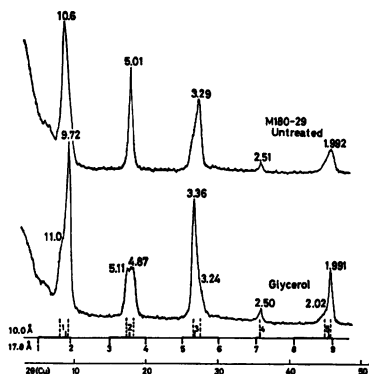


FIG. 5. X-ray diffraction patterns of specimen M180-29 (oriented aggregate).

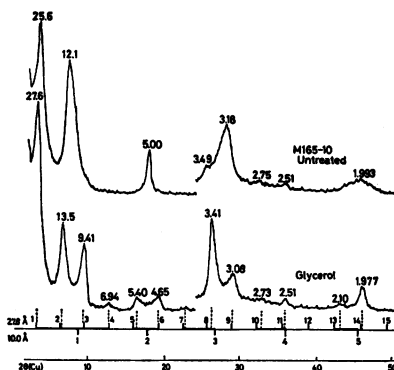


FIG. 6. X-ray diffraction patterns of specimen M165-10 (oriented aggregate).

The last specimen M165-10 gives a long spacing reflection, indicating that the specimen comes within the category of regular interstratification. After the glycerol treatment the 25.6 Å reflection shifts to 27.6 Å, and the number of higher order reflections increases (Fig. 6). The basal reflections do not appear at exactly integral submultiples of the 001 spacings. The shifts after glycerol solvation suggest that a few additional mica layers are randomly interstratified with the regularly interstratified system of mica and montmorillonite, as shown in the lower part of the same figure.

A Fourier transform method after MacEwan (1956) was applied to the x-ray pattern of specimen M165-10 in order to obtain direct information on the nature of interstratification. The average values of the structure factor used in this method were read from the tabular data of Cole and Launciki (1966). Fig. 7 shows the result for the glycerol treated specimen, where A represents the mica layer (10 Å) and B the expanded montmorillonite layer (18 Å). This pattern indicates a tendency of alternation of two different layers. The quantity ratio of mica to montmorillonite 60:40 was

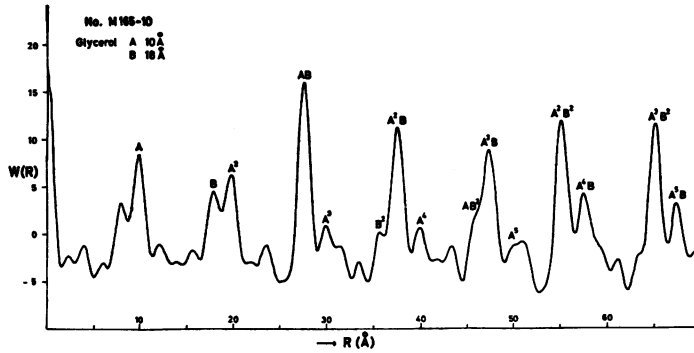


FIG. 7. Fourier transform of basal reflections of glycerol-treated specimen M165-10.

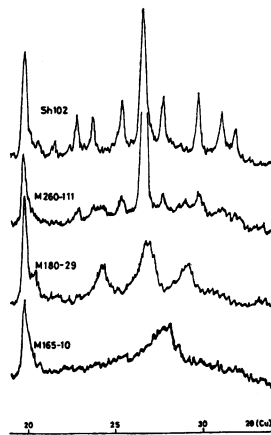


FIG. 8. X-ray diffraction patterns of sericite minerals (random powder).

obtained from the heights of peaks A and B.

Fig. 8 shows x-ray diffraction patterns of some randomly oriented specimens. The x-ray patterns of specimens Sh102 and M180-29 (all reflections of the latter are broadened because of intermixing of the montmorillonite layer) are typical ones of the $2M_1$ and $1M$ polytypes, respectively. The peaks of both the $1M$ and $2M_1$ polytypes are recognized in the x-ray pattern of specimen M260-111, although the hkl reflections are very weak as compared with the basal reflections. Specimen M165-10 has no distinct hkl reflections and belongs to $1Md$.

CHEMICAL COMPOSITION

Chemical analysis was carried out by a wet standard method. The results are listed in Table 2 together with the structural formulae. The pre-

TABLE 2. Chemical compositions and structural formulae of sericite minerals

	M260-111	Sh102	K328-03	K329-12	M180-29	M165-10
SiO ₂	48.76	46.47	47.21	46.83	49.86	48.88
TiO ₂	0.83	0.50	0.85	1.13	0.49	0.73
Al ₂ O ₃	32.33	37.34	36.18	33.10	32.25	31.35
Fe ₂ O ₃	1.29	0.20	0.29	0.97	0.15	0.33
MgO	1.78	0.46	0.58	1.14	1.43	0.97
CaO	0.17	0.09	0.13	0.23	0.37	0.54
Na ₂ O	0.21	0.37	0.75	0.89	0.31	0.92
K ₂ O	9.71	8.85	8.17	7.42	7.96	5.12
H ₂ O ⁺	5.65	5.54	5.68	6.17	6.25	7.58
H ₂ O ⁻	0.34	0.49	0.74	1.59	1.72	3.67
Total	100.62	100.31	100.58	99.47	100.79	100.09
Tetrahedral						
Si	3.25	3.08	3.14	3.20	3.33	3.37
Al	0.75	0.92	0.86	0.80	0.67	0.63
Charge	-0.75	-0.92	-0.86	-0.80	-0.67	-0.63
Octahedral						
Al	1.78	1.99	1.97	1.87	1.87	1.91
Fe ³⁺	0.06	0.01	0.02	0.05	0.00	0.02
Mg	0.18	0.04	0.05	0.12	0.14	0.10
Sum	2.02	2.04	2.04	2.04	2.01	2.03
Charge	-0.12	+0.08	+0.07	0.00	-0.11	-0.01
Interlayer						
Ca	0.01	0.01	0.01	0.02	0.03	0.04
Na	0.03	0.05	0.10	0.12	0.04	0.12
K	0.82	0.75	0.69	0.65	0.68	0.45
Charge	+0.87	+0.82	+0.81	+0.81	+0.78	+0.65

sent specimens are characterized by the high alumina content, and the very low magnesium and iron contents. The silica content varies within a narrow range. Distinct variations in the potassium and minus water contents caused by the differences in the content of montmorillonite layers are recognized.

The structural formulae were calculated on the basis of O₁₀(OH)₂. The sum of the number of octahedral cations is very close to 2.0 for all specimens, indicating the dioctahedral structure of the minerals. The number of iron and magnesium atoms varies subtly from specimen to specimen, and the substitution of these atoms for aluminium affects some properties of the minerals as shown in the later sections.

From these results, it is concluded that the present specimens are chemically composed of dioctahedral mica (sericite) and dioctahedral montmorillonite.

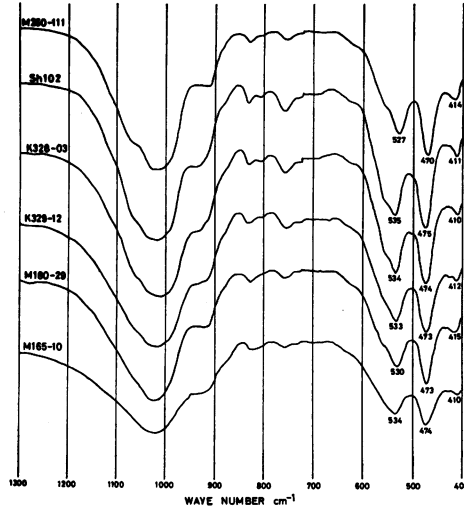


FIG. 9. Infrared absorption spectra of sericite minerals.

INFRARED ABSORPTION ANALYSIS

The finely powdered 0.5 mg specimen was mixed with 300 mg of KBr, and was pressed into a disc. Measurements were made with a Hitachi EPI-G grating spectrophotometer in the spectral region between 400 and 4000 cm^{-1} . The infrared absorption spectra obtained are given in Fig. 9. There is a systematic variation in the absorption spectra of the minerals which is related with their chemical composition.

Stubican and Roy (1961) studied the infrared spectra of synthetic muscovite-phengite series and demonstrated that by substitution of magnesium for octahedral aluminium the absorption band at about 530 cm^{-1} shifts towards lower frequencies and simultaneously the band at 930 cm^{-1} becomes poorly

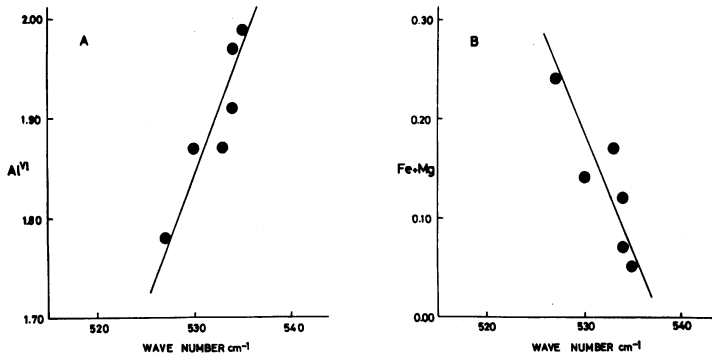


FIG. 10. Relationships between the frequency of the 530 cm^{-1} band and the number of octahedral cations, Al (A) and Fe + Mg(B), per $\text{O}_{10}(\text{OH})_2$ unit of sericite minerals.

defined. As shown in Fig. 10, linear relations between the frequency of the 530 cm^{-1} band and the number of the octahedral cations are observed for the present specimens, which agrees with the result of Stubican and Roy. The band around 410 cm^{-1} also shifts by substitution of the octahedral cations.

The double absorption peaks in the region of $800\text{--}830\text{ cm}^{-1}$ of specimens Sh102 and K328-03 may indicate that they are $2M_1$ polytypes, and the single peak of specimen M180-29 at 800 cm^{-1} that it is $1M$ polytype (Oinuma and Hayashi, 1965). Specimens M260-111 and K329-12 give intermediate spectra of the two polytypes, suggesting that they are mixtures of the $1M$ and $2M_1$ polytypes. These results agree with those of x-ray analysis.

DIFFERENTIAL THERMAL ANALYSIS

Differential thermal analysis curves given in Fig. 11 were recorded on a Shimadzu micro DTA apparatus using 20 mg of specimen. Heating rate was

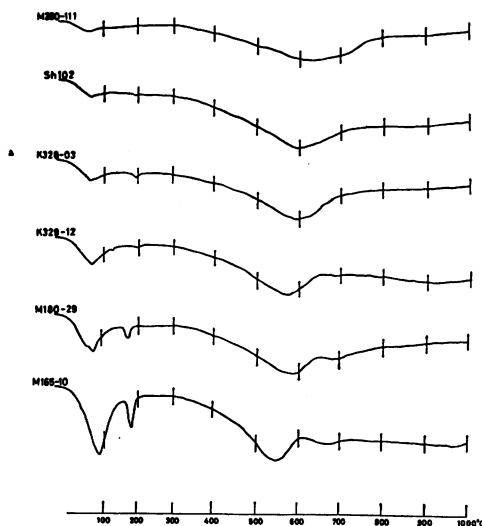


FIG. 11. Differential thermal analysis curves of sericite minerals.

10°C per minute. There occur two endothermic peaks due to removal of interlayer water (under 200°C) and structural OH (between 500°C and 700°C). The size of the endothermic peak due to removal of interlayer water is correlated to the proportion of montmorillonite layer in the specimen. On the other hand, the appearance of the peaks due to removal of structural OH seems to be related to the octahedral composition: the specimens with exclusively high aluminium contents (Sh 102 and K 328-03) show a single endothermic peak, and those with relatively high magnesium and iron contents (M180-29 and M165-10) double ones. Specimen M260-111, containing the highest amounts of magnesium and iron, shows a shallow and broad

peak extending up to 700 °C, which may be comparable with the double peaks.

The differential thermal analysis curves of interstratified minerals of mica and montmorillonite were considered to have retained the character of the mineral from which the interstratified mineral was formed, and the pre-existing mineral was inferred (Cole and Hosking, 1957; Shimoda and others, 1969; Shimoda, 1972). In the case of the present specimens, the differences in the endothermic reactions due to dehydroxylation rather seems to reflect the difference of chemical composition of these materials. Many infrared and DTA data for sericite minerals other than the present specimens also support the latter interpretation (Shirozu and Higashi, unpublished).

CONCLUDING REMARKS

The analytical results for six specimens are summarized in Table 3. The values of $d(060)$ were measured by using silicon powder as an internal standard.

TABLE 3. Variations in polytype, $d(060)$, 530 cm^{-1} band frequency and octahedral composition of six specimens

Specimen	Polytype	$d(060)$ Å	530 cm^{-1} band frequency cm^{-1}	Octahedral composition
M260-111	$2M_1+1M$	1.502	527	$\text{Al}_{1.78}\text{Fe}_{0.06}\text{Mg}_{0.18}$
Sh 102	$2M_1$	1.498	535	$\text{Al}_{1.99}\text{Fe}_{0.01}\text{Mg}_{0.04}$
K328-03	$2M_1$	1.498	534	$\text{Al}_{1.97}\text{Fe}_{0.02}\text{Mg}_{0.05}$
K329-12	$2M_1+1M$	1.499	533	$\text{Al}_{1.87}\text{Fe}_{0.05}\text{Mg}_{0.12}$
M180-29	1M	1.500	530	$\text{Al}_{1.87}\text{Fe}_{0.00}\text{Mg}_{0.14}$
M165-10	1Md	1.497	534	$\text{Al}_{1.91}\text{Fe}_{0.02}\text{Mg}_{0.10}$

Table 3 demonstrates that the values of $d(060)$ and the frequency of the 530 cm^{-1} band which vary in the ranges of 1.497-1.502 Å and 527-535 cm^{-1} , respectively, depend mainly on the octahedral composition, and that this compositional variation is also related to the polytype. Namely, the polytype is $2M_1$ when the composition of the mineral is close to that of muscovite but it is 1M when the composition of the mineral is relatively distant from that of muscovite on account of the octahedral magnesium and iron substitution. This trend is also shown in Fig. 12, which is a celadonite-muscovite-pyrophyllite diagram after Hower and Mowatt (1966). The present specimens are plotted in this diagram together with sericite minerals from literature. The compositions of the $2M_1$ specimens (open circles) which fall close to that of muscovite, are apparently distinguished from those of the 1M specimens (closed circles) with relatively low tetrahedral

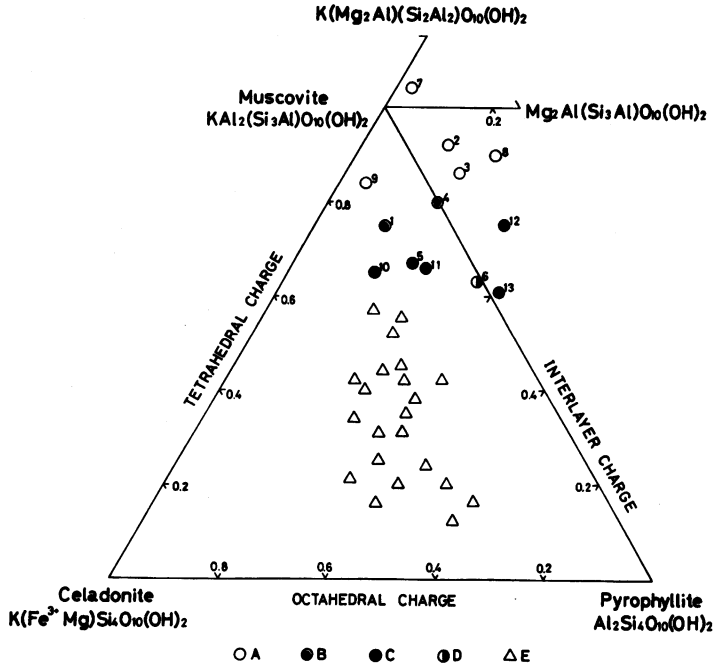


FIG. 12 Distribution of sericite mineral compositions in the composition triangle diagram of celadonite-muscovite-pyrophyllite.

A, $2M_1$; B, $2M_1+1M$; C, $1M$; D, $1Md$; E, Illite-montmorillonite series (Hower and Mowatt, 1966).

1. Specimen M260-111, this paper.
2. Specimen Sh102, this paper.
3. Specimen K328-03, this paper.
4. Specimen K329-12, this paper.
5. Specimen M180-29, this paper.
6. Specimen M165-10, this paper.
7. Siwati, Hiroshima Pref. (Yamamoto, 1967).
8. Shakanai mine, Akita Pref. This specimen was described as $2M_2$ by Shimoda (1970).
9. Goto mine, Nagasaki Pref. (Shimoda and others, 1969).
10. Hanaoka mine, Akita Pref. (Shimoda and others, 1969).
11. Kamikita mine, Aomori Pref. (Shimoda and others, 1969).
12. Kurosawa mine, Fukushima Pref. (Shimoda and others, 1969).
13. Iwami mine, Shimane Pref. (Shimoda and others, 1969).

charges.

Hower and Mowatt (1966) investigated illite and interstratified illite-montmorillonite in sedimentary rocks, and demonstrated that the proportion of montmorillonite layer has a good correlation with the interlayer charge of the mineral. For the present specimens, this correlation is not so distinct. A notable fact is that the compositional difference between $1M$ sericite and

illite with no expandable layer component is very small, but it becomes large when considerable amounts of expandable layer components are intermixed. This fact may correspond to the genetic difference between these sericite minerals and the illite-montmorillonite series. However, in order to clarify these relationships, more detailed investigations of other specimens are required.

ACKNOWLEDGMENTS

The author wishes to express his sincere thanks to Professor Haruo Shirozu of Kyushu University for many helpful suggestions during the course of this study and for critical reading of the manuscript. Hearty thanks are due to Dr. Kiyoshi Ishibashi of Kyushu University and Dr. Masaharu Ozaki of Kumamoto University for their kind advice on the chemical analysis. Finally, the author should like to record his hearty thanks to Mr. Takeshi Date of Furukawa Mining Co. Ltd. who collected some specimens used in this study. A part of this study was financed by the Grant in Aid of Scientific Research from the Ministry of Education.

REFERENCES

- COLE, W. F. and HOSKING, J. S. (1957) *Differential Thermal Investigation of Clays* (ed. by Mackenzie, R. C.), chap. 5, 248-274.
- COLE, W. F. and LAUNCIKI, C. J. (1966) *Acta Cryst.*, **21**, 836-838.
- HOWER, J. and MOWATT, T. C. (1966) *Am. Mineral.*, **51**, 825-854.
- MACEWAN, D. M. C. (1956) *Kolloid-Zs.*, **149**, 96-108.
- MACEWAN, D. M. C., RUIZ AMIL, A. and BROWN, G. (1961) *The X-ray Identification and Crystal Structures of Clay Minerals* (ed. by Brown, G.), chap. 11, 393-445.
- OINUMA, K. and HAYASHI, H. (1965) *Am. Mineral.*, **50**, 1213-1227.
- SHIMODA, S. (1970) *Clays and Clay Miner.*, **18**, 269-274.
- SHIMODA, S. (1972) *Clay Sci.*, **4**, 115-125.
- SHIMODA, S., SUDO, T. and OINUMA, K. (1969) *Proc. Intern. Clay Conf.*, **1969, Tokyo**, **I**, 197-206.
- SHIMODA, S. and NISHIYAMA, T. (1973) *Nendo Kagaku*, **13**, 48-54 (in Japanese).
- SHIROZU, H. and HIGASHI, S. (1972) *Clay Sci.*, **4**, 137-142.
- SHIROZU, H., DATE, T. and HIGASHI, S. (1972) *Min. Geol. (Tokyo)*, **22**, 393-402 (in Japanese).
- STUBICAN, V. and ROY, R. (1961) *Am. Mineral.*, **46**, 32-51.
- WEAVER, C. E. (1956) *Am. Mineral.*, **41**, 202-221.
- YAMAMOTO, T. (1967) *Mineral. Jour.*, **5**, 77-97.